

A fast model for THM processes in geothermal applications

Peter A. Fokker^{1, 2} and Brecht B.T. Wassing¹

¹ TNO Applied Geosciences, Utrecht The Netherlands

² Utrecht University, Utrecht, The Netherlands

peter.fokker@tno.nl

Keywords: Enhanced Geothermal Systems, Coupled modelling; Stimulation.

ABSTRACT

We have developed a fast modelling tool, THYMA, for coupled poro-thermo-elastic-plastic behaviour. The tool targets data assimilation and optimization of geothermal operations, like stimulation. A validation with coupled numerical model yielded positive results for elastic responses to the a pressure increase; the implementation and validation of plasticity is in progress..

1. INTRODUCTION

Coupled processes are essential in geothermal applications: in low-permeability reservoir the heat that is to be harvested can only materialize when enough flow capacity is present, requiring mechanical stimulation. In such a setting, the interpretation of measurements and the optimization of operations require fast models that allow ensemble methods running multiple realizations of parameter choices and operational constraints.

We report here the development of a model targeted at such applications. It extends an existing hydro-mechanical model to also include thermoelasticity and account for fluid mobility changes with changing temperature. Axial symmetry of the flow is assumed. We demonstrate the accuracy of the model by calibration against a coupled numerical code.

2. MODEL

The target of the present investigation is the mechanical response of injection or production in geothermal wells, and its consequences for injectivity, wellbore stability and seismicity potential. In the present paper we limit ourselves to radial symmetry and an isotropic far-field horizontal stress.

Linear poro-thermo-elasticity involves a linear relationship between stress σ_{ij} , strain ε_{ij} , and increases in pore pressure (ΔP) and temperature (ΔT) (Palciauskas & Domenico, 1982):

$$\sigma_{ij} = 2G \left[\varepsilon_{ij} + \frac{\nu}{1-2\nu} \varepsilon \delta_{ij} \right] - (\alpha_b \Delta P + \beta_T \Delta T) \delta_{ij} + \sigma_{ij}^\infty \quad [1]$$

Stress equilibrium gives, in a radial symmetry

$$\frac{\partial \sigma_{rr}}{\partial r} + \frac{\sigma_{rr} - \sigma_{\theta\theta}}{r} = 0 \quad [2]$$

When this is coupled to a mass balance equation and a linear relationship between pressure gradient and flow velocity (Darcy flow) in a constant-mobility reservoir, we arrive at a diffusivity equation for the pressure in the reservoir (Detournay and Cheng, 1995).

Since we are interested in the effect of temperature changes and stimulation, the analytical solution of the diffusivity equation cannot be used. Instead, we employ a semi-steady-state solution that is applicable close to the well: within the radius where the pressure is disturbed, we have

$$\frac{dp}{dr} = - \frac{Q_{inj}}{2\pi\lambda hr} \quad [3]$$

For the temperature disturbance, we employ an energy balance approach: the (negative) thermal energy introduced by injection must equal the thermal energy of a cooled zone around the wellbore – assuming a step-change between the cooled and the non-cooled regions and no thermal diffusion to layers above and below the reservoir.

The requirement of permeability and temperature updates has led us to a time stepping approach.

The initial solution, in which no pressure and temperature disturbances are present, is the well-known solution for stresses around an open borehole. In a field with isotropic horizontal stresses, we have

$$\begin{aligned} \sigma_{rr} &= \sigma_h^\infty - \frac{Z_1^0}{r^2} \\ \sigma_{\theta\theta} &= \sigma_h^\infty + \frac{Z_1^0}{r^2} \\ \sigma_{zz} &= \sigma_z^\infty \end{aligned} \quad [4]$$

The integration constant Z_1^0 is controlled by the inner boundary condition that the radial stress at the wellbore must cancel the wellbore pressure (we use the engineering convention of negative sign for compressive normal stress). A second integration constant (a constant Z_2^0 to be added to the horizontal stresses) is zero in the present formulation because of the boundary condition at infinity.

For later times the pressure and temperature fields are used to update the stress field with a linear poro-thermo-elastic contribution.

For failure we employ a common approach with the Coulomb failure criterion (Jaeger, Cook and Zimmerman, 2007). Failure will occur along a plane if the following condition is satisfied for the shear stress τ and the effective normal stress σ' :

$$|\tau| = S_0 - \mu\sigma' \quad [5]$$

For the effective stress for plasticity we use the Terzaghi definition, $\sigma_{ij}^{\prime pl} = \sigma_{ij} + P\delta_{ij}$.

If the plane of failure is not pre-determined, failure will occur when the Mohr circle touches the failure envelope. This condition can be translated to a relationship between the maximum and minimum effective principal stresses, $\sigma_1^{\prime pl}$ and $\sigma_3^{\prime pl}$ (Jaeger, Cook & Zimmermann, 2009; Fjaer et al, 2007):

$$\begin{aligned} \sigma_1^{\prime pl} &= -2S_0\Gamma + \gamma\sigma_3^{\prime pl} \\ \Gamma &= \frac{\cos\phi}{1-\sin\phi} \\ \gamma &= \Gamma^2 = \frac{1+\sin\phi}{1-\sin\phi} \end{aligned} \quad [6]$$

This condition is used to assess whether the elastic solution is applicable for the complete region.

Now for the plastic zone we assume that the stress is at the failure line (Han and Dusseault, 2003; Masoudian and Hashemi, 2016). In case the tangential stress is largest (i.e. the absolute value of the tangential stress is the largest one, $\sigma_{\theta\theta} = \sigma_1$), we can introduce the relationship between the plastic stresses and the expression for the pressure gradient in the equilibrium equation, to arrive at

$$\frac{d\sigma_{rr}'}{dr} - (\gamma - 1)\frac{\sigma_{rr}'}{r} = -\frac{1}{r}\left[\frac{Q_{inj}}{2\pi\lambda h} + 2S_0\Gamma\right] \quad [7]$$

This differential equation can be solved, giving horizontal plastic compressive effective stresses as

$$\begin{aligned} \sigma_{rr} &= -\Delta P(r) + r^{\gamma-1}\left\{r_A^{1-\gamma}[\sigma_{rr}^A + \Delta P^A] - \int_{r_w}^r \left[\frac{Q_{inj}}{2\pi\lambda h} + 2S_0\Gamma\right] \frac{d\rho}{\rho^\gamma}\right\} \\ \sigma_{\theta\theta} &= -\Delta P(r) - 2S_0\Gamma + \gamma\sigma_{rr}' \end{aligned} \quad [8]$$

The integration constant σ_{rr}^A is found through the inner boundary condition of vanishing effective stress at the wellbore,

The strain increase in the plastic regime is composed of an elastic and a plastic part:

$$\delta\varepsilon_{ij} = \delta\varepsilon_{ij}^e + \delta\varepsilon_{ij}^p \quad [9]$$

We employ a non-associated flow rule to find the displacement in the plastic regime (Masoudian and Hashemi, 2016). The radial and tangential components are related through the dilation angle ψ as

$$\delta\varepsilon_{rr}^p + \beta\delta\varepsilon_{\theta\theta}^p = 0$$

$$\beta = \frac{1+\sin\psi}{1-\sin\psi} \quad [10]$$

Now, for radial symmetry, we have

$$\delta\varepsilon_{rr} = \frac{\partial\delta u}{\partial r}; \quad \delta\varepsilon_{\theta\theta} = \frac{\delta u}{r} \quad [11]$$

And we can write for the total strain

$$\frac{\partial\delta u}{\partial r} + \beta\frac{\delta u}{r} = f(r) \quad [12]$$

The function $f(r)$ depends on the incremental elastic strain only, and can thus be calculated using the linear poro-thermo-elastic response to the plastic stress. The differential equation can be solved as

$$\delta u(r) = u_A\left(\frac{r}{r_A}\right)^{-\beta} + r^{-\beta} \int_{r_A}^r \rho^\beta f(\rho) d\rho \quad [13]$$

In the case that part of the domain is reacting plastically, the plastic and elastic domains must be connected. Interface conditions are required on top of the usual boundary conditions at the wellbore and in infinity. For every zone we have a solution with two integration constants: Z_1 and Z_2 in the elastic domain; u_A and σ_{rr}^A for the plastic domain. Further, the radius of the plastic zone is yet undetermined.

The conditions to match the solutions are

- Horizontal stresses at infinity equal the virgin horizontal stress
- Radial stress at the wellbore is compensated by the wellbore pressure
- The radial stress at the elastic-plastic interface is continuous
- The displacement at the elastic-plastic interface is continuous
- The relationship between tangential and radial elastic stress at the interface is such that the failure criterion is just reached.

The solutions and the conditions allow the formulation of the mechanical solution. At the end of a timestep, the fields have been updated with respect to the timestep before. This allows to also update the permeability field. Either a stress-dependent permeability can be used or the dilation can be calculated and used as input in a porosity – permeability relationship or in an effective fracture network.

3. VALIDATION

The above correlations have been implemented in a software tool, which has been coined THYMA (Thermo-Hydro-Mechanic Analysis). At every timestep, the only numerical treatment is a routine to find the elastic-plastic transition radii. As a result, calculations are very fast; in the order of seconds CPU for hundreds of timesteps.

We have used a coupled FLAC – TOUGH model to validate findings with THYMA. The FLAC – TOUGH

tool is described in a companion paper (Wassing et al, 2019).

The case that we study is a synthetic case considered typical for geothermal injection in homogeneous rock. We inject $4 \cdot 10^{-3} \text{ m}^3/\text{s}$ in a 10 m thick reservoir with a permeability of $2 \cdot 10^{-14} \text{ m}^2$. Further details are provided in Table 1. At this stage of the investigation we have not yet investigated the effect of changing permeability. Also, the effect of temperature has not yet been investigated in detail.

Table 1: Reservoir and flow parameters for the validation cases

Table values	Fully Elastic	With plastic region
Reservoir thickness	10 m	
Wellbore radius	1 m	
Water injection rate	$4 \cdot 10^{-3} \text{ m}^3/\text{s}$	
Duration of injection	$2.59 \cdot 10^6 \text{ s}$ (30 days)	
Water viscosity	0.34 mPa.s	
Water bulk modulus	4.25 GPa	
Young's modulus	15 GPa	
Reservoir Poisson ratio	0.20	
Biot factor	1.0	
Reservoir permeability	$2.0 \cdot 10^{-14} \text{ m}^2$ (20 md)	
Reservoir porosity	0.20	
Initial reservoir pressure	25 MPa	
Far-field horizontal stress	40 MPa	
Far-field vertical stress	40 MPa	
MC friction coefficient	0.57	
MC cohesion	10 GPa	2 MPa

Figure 1 presents the match between the pore pressure results as obtained with THYMA and with FLAC – TOUGH. We had to increase the water bulk modulus to a large value (4.25 GPa instead of 2.5 GPa) to obtain a good fit – this is presumably related to a suboptimal treatment of fluid diffusion in TOUGH2. Still, the figure shows that the approximation of a moving pressure front into the formation is accurate when the diffusivity can be matched.

Figure 2 presents the elastic stresses before the pressure is disturbed. The traces represent the well-known stress solution for isotropic far-field stresses. For the case where part of the reservoir reacts plastically, the results of the initial stresses, before disturbing with the pressure, are given in Figure 3. The excellent agreement is a validation of the concept of a plastic-elastic transition on which the radial stress and the displacement must be continuous, while the elastic tangential stress must approach the failure envelope and further the usual boundary conditions at the wellbore and at infinity must be adhered.

The development of the stresses versus time is presented in Figure 4 and Figure 5. The figures show excellent agreement. One note must here be made, however: the calculations with the plastic behaviour

included do not reach plasticity again in the interior of the reservoir. Also, the extensional stresses that develop close to the wellbore when deploying THYMA are not represented in FLAC – TOUGH. The latter is related to the FLAC settings with regard to extensional stresses. As the reader will appreciate, this is subject of investigation at the time of writing the present document.

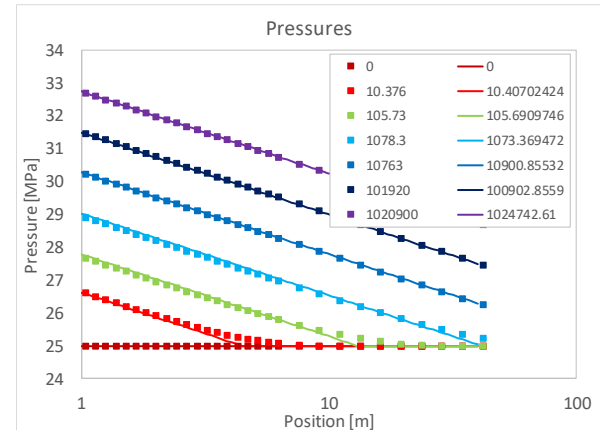


Figure 1: Pressures vs position for various times since start. Symbols: FLAC – TOUGH. Lines: THYMA. Legend: Times (in s).

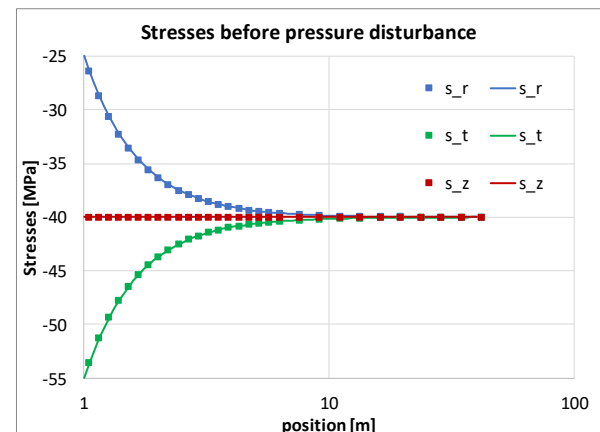


Figure 2: Stresses vs position before start, for the elastic case. Symbols: FLAC – TOUGH. Lines: THYMA.

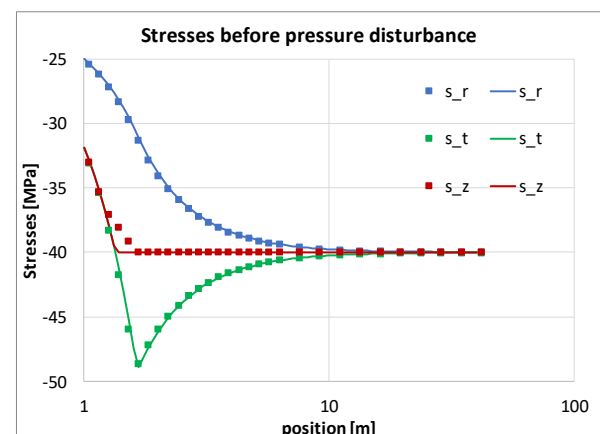


Figure 3: Stresses vs position before start, for the plastic case. Symbols: FLAC – TOUGH. Lines: THYMA.

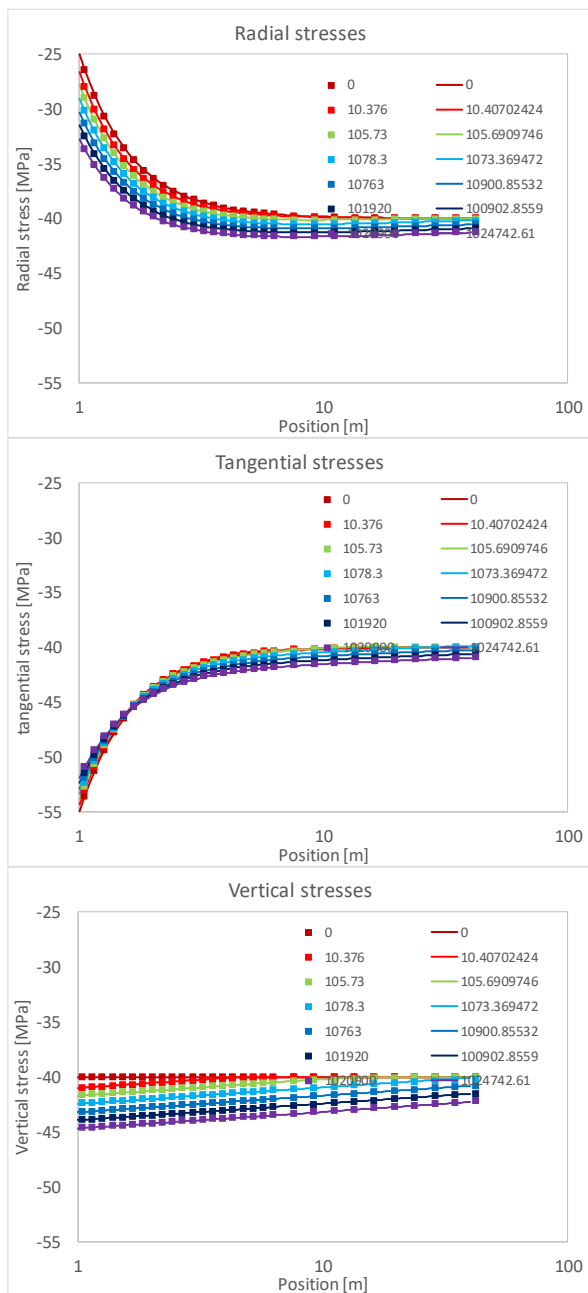


Figure 4: Stress development vs position for the elastic case. Symbols: FLAC – TOUGH. Lines: THYMA. Top: radial stress; Middle: Tangential stress; Bottom: Vertical stress

4. DISCUSSION AND CONCLUSION

We have invented, implemented and validated a fast modelling tool, THYMA, for coupled poro-thermo-elasto-plastic behaviour. The implementation of the development of plasticity is in progress.

Further developments are important to make THYMA more widely applicable. Extensions will be pursued in the direction of actual implementation of permeability enhancement, validation of the effect of cooling,

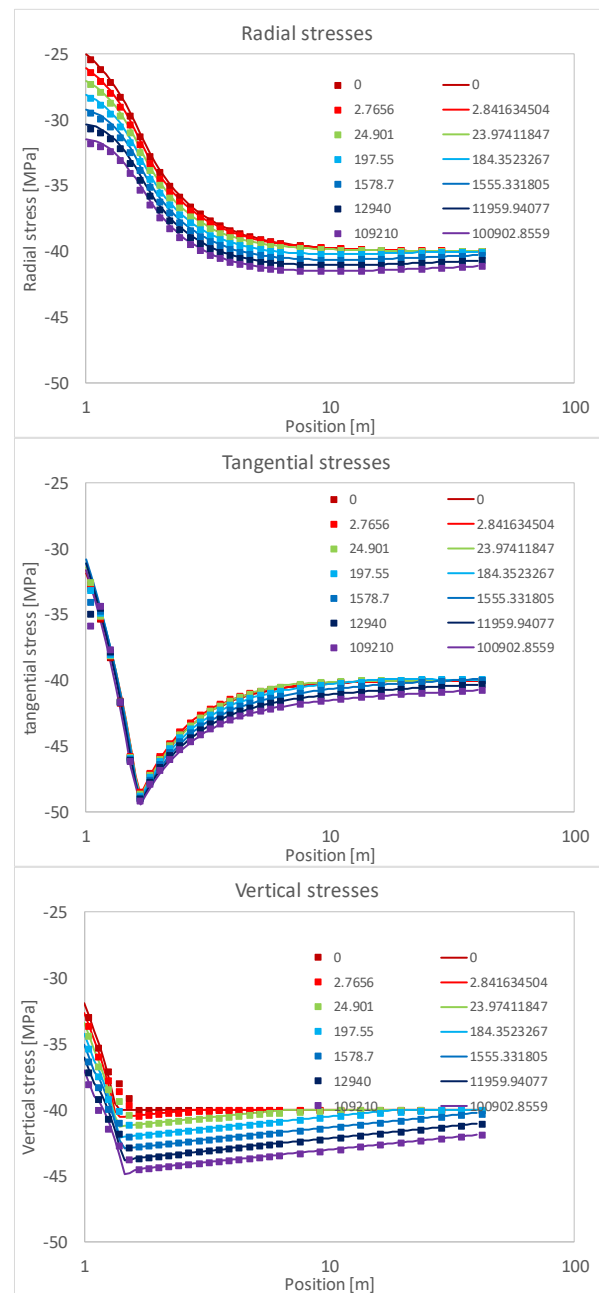


Figure 5: Stress development vs position for the plastic case. Symbols: FLAC – TOUGH. Lines: THYMA. Top: radial stress; Middle: Tangential stress; Bottom: Vertical stress

anisotropic far-field horizontal stresses, the effect of finite height, and alternative failure criteria.

REFERENCES

Detournay, E., and Cheng, A. H. D.. Fundamentals of poroelasticity. In *Analysis and design methods* (1995) (pp. 113-171).

Fjaer, E., Horsrud, P., Raaen, A. M., Risnes, R., & Holt, R. M.. *Petroleum related rock mechanics* (Vol. 33). Elsevier (2007).

- Han, G., and Dusseault, M. B.. Description of fluid flow around a wellbore with stress-dependent porosity and permeability. *Journal of Petroleum science and engineering*, 40(1-2) (2003), 1-16.
- Jaeger, J. C., Cook, N. G., and Zimmerman, R.. *Fundamentals of rock mechanics*. John Wiley & Sons (2007).
- Masoudian, M.S., and Hashemi, M.A.. Analytical solution of a circular opening in an axisymmetric elastic-brittle-plastic swelling rock. *Journal of Natural Gas Science and Engineering*, 35 (2016), 483-496.
- Palciauskas, V. V., and Domenico, P. A.. Characterization of drained and undrained response of thermally loaded repository rocks. *Water Resources Research*, 18(2), (1982) 281-290.
- Wassing, B.B.T., Gan, Q., Candela, T.G.G., Loeve, D. and Fokker, P.A. Modelling the effect of hydraulic stimulation strategies on fault reactivation and induced seismicity. *Eur. Geothermal Congress 2019*, Den Haag, The Netherlands, 11-14 June 2019.

Acknowledgements

The project leading to the results in this article received funding from the European Union's Horizon 2020 research and innovation programmes under grant agreement No 691728 and under grant agreement No. 727550.